Original article

MOLECULAR METABOLISM

^{11}C-meta-hydroxyephedrine PET/CT imaging allows *in vivo* study of adaptive thermogenesis and white-to-brown fat conversion

Carmelo Quarta [1,4,*], Filippo Lodi [2], Roberta Mazza [1], Ferdinando Giannone [3], Laura Boschi [2], Cristina Nanni [4], Enzo Nisoli [5], Stefano Boschi [2], Renato Pasquali [1], Stefano Fanti [4], Patricia Iozzo [6], Uberto Pagotto [1]

ABSTRACT

Several lines of evidence suggest that novel pharmacological approaches aimed at converting white adipose tissue (WAT) into brown adipose tissue (BAT) may represent an effective therapeutic strategy for obesity and related disorders. $^{(18)}$F-fluorodeoxyglucose (^{18}F-FDG) is the only positron emission tomography (PET) tracer commonly used to study BAT function, and so far no functional tools have been described to investigate *in vivo* white-to-brown fat conversion. In this report, we show that the PET tracer ^{11}C-meta-hydroxyephedrine (^{11}C-MHED, a norepinephrine analogue) is a useful tool to investigate the sympathetic nervous system (SNS) activity in BAT of lean and dietary obese mice. Moreover, we demonstrate that ^{11}C-MHED is a specific marker of the SNS-mediated thermogenesis in typical BAT depots, and that this tracer can detect *in vivo* WAT to BAT conversion.

Keywords Brown adipose tissue; Sympathetic activity; PET/CT imaging

1. INTRODUCTION

The key role played by brown adipose tissue (BAT) in the regulation of energy balance in mammals has been known for decades [1,2]. A high number of mitochondria and the presence of the uncoupling protein 1 (UCP-1) give brown adipocytes the ability to control the metabolic efficiency in rodents [3]. Moreover, increasing evidence indicates that stimulation of BAT thermogenesis promotes whole body energy dissipation and improves the metabolic profile in animal models of obesity [4–6]. Therefore, molecules able to activate BAT thermogenesis may have beneficial effects in obesity and related disorders. Hybrid PET/CT imaging has recently demonstrated the presence of metabolically active brown fat in adult humans [7–9]. However, it is unclear whether the small amount of BAT found in adult individuals can significantly influence whole body energy metabolism. Therefore, the possibility to increase BAT amount by promoting white adipose tissue (WAT)-to-brown fat conversion has become a hot research topic in recent years. Several investigations have reported that white adipocytes can transdifferentiate into brown adipocytes when appropriately stimulated [10,11]. Moreover, several transcription factors and endocrine regulators of brown adipocyte differentiation and function have been identified [12].

To date, non-invasive tools to detect and measure the degree of WAT to BAT conversion are lacking, though PET/CT imaging of $^{(18)}$F-fluorodeoxyglucose (^{18}F-FDG) has been commonly used to investigate interscapular BAT metabolism. The sympathetic nervous system (SNS) is a key regulator of BAT thermogenesis [2] and of brown fat cell differentiation and proliferation [10]. Some PET tracers can provide specific norepinephrine (NE)-related signals in BAT [13,14]. However, the potential use of PET/CT imaging of SNS activity for the analysis of BAT thermogenesis has not been fully evaluated.

In this report, we examined whether PET/CT imaging of ^{11}C-meta-hydroxyephedrine (^{11}C-MHED, a positron emitting NE analogue) may be a suitable technique to measure *in vivo* SNS-mediated thermogenesis in BAT. We analyzed ^{11}C-MHED uptake in the interscapular BAT (iBAT) of lean and diet-induced obese (DIO) mice during activation or blockade of SNS-mediated thermogenesis. Moreover, to study whether PET/CT imaging makes it possible to detect and quantify the metabolic activity of brown adipose cells that are generated *de novo* in WAT, we analyzed ^{11}C-MHED and ^{18}F-FDG uptake in WAT of mice chronically treated with a β_3-adrenergic receptor (β_3AR) agonist, *i.e.* an approach known to promote WAT to BAT conversion.

2. RESULTS

2.1. *In vivo* ^{11}C-MHED bio-distribution in BAT

As shown in Figure 1a, PET/CT imaging allowed a clear detection of ^{11}C-MHED avid areas in the iBAT. With preliminary experiments, we had found that gas anesthesia administration (sevorane with 1% of oxygen supplementation) profoundly affects ^{11}C-MHED uptake in BAT (data not shown). Therefore, to characterize the time-dependent bio-distribution of

[1]Endocrinology Unit and Center for Applied Biomedical Research, Department of Medical and Surgical Sciences, University of Bologna, Bologna 40138, Italy [2]PET Radiopharmacy, Nuclear Medicine Unit, S. Orsola-Malpighi Hospital, Bologna 40138, Italy [3]Department of Clinical Medicine, U.O. Semeiotica Medica, and Center for Applied Biomedical Research, University of Bologna, Bologna 40138, Italy [4]Department of Nuclear Medicine, S. Orsola-Malpighi Hospital, University of Bologna, Bologna 40138, Italy [5]Integrated Laboratories Network, Center for Study and Research on Obesity, Department of Medical Biotechnology and Translational Medicine, University of Milan, Milan 20129, Italy [6]Institute of Clinical Physiology, National Research Council (CNR), 56124 Pisa, Italy

*Corresponding author at: University of Bologna, Department of Medical and Surgical Sciences, Endocrinology Unit and Center for Applied Biomedical Research, CRBA, Pad 20, Via Massarenti, 9, Policlinico S. Orsola-Malpighi, 40138 Bologna, Italy. Tel.: +49 1511095758. Email: quartacarmelo@yahoo.it (C. Quarta)

Received March 21, 2013 • Revision received April 6, 2013 • Accepted April 8, 2013 • Available online 21 April 2013

http://dx.doi.org/10.1016/j.molmet.2013.04.002

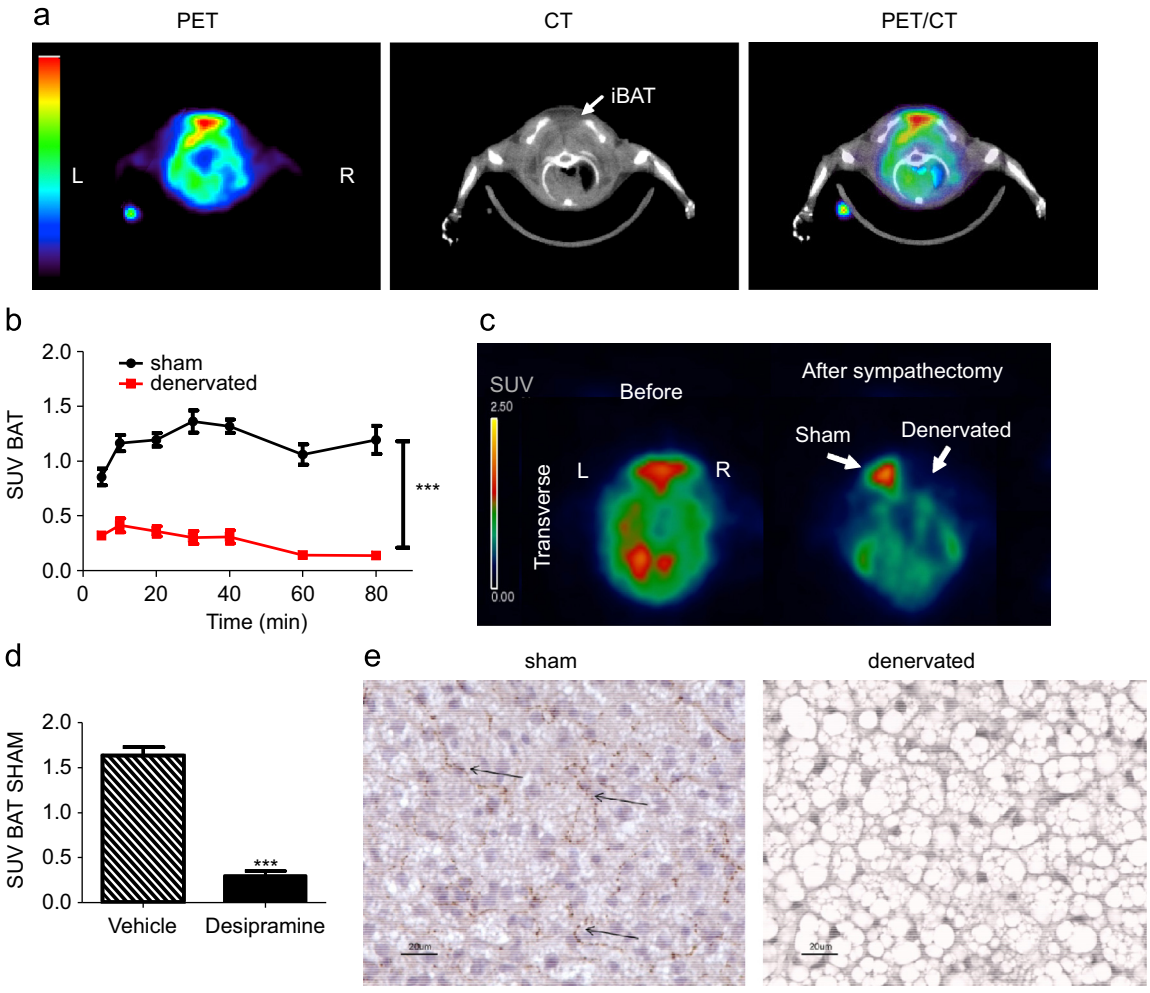

Figure 1: Analysis of ^{11}C-MHED bio-distribution in BAT. See also Figure S1. (a) Transverse views of PET (left), CT (middle), and PET/CT fused (right) images showing ^{11}C-MHED uptake in the iBAT (arrow) of a representative mouse. L: left and R:right. (b) PET/CT analysis of the time-course of ^{11}C-MHED distribution in SNS-denervated ($n=6$) or sham-operated ($n=6$) iBAT depots of C57BL/6 mice analyzed by several repeated PET/CT scans. $^{**}p < 0.005$, $^{***}p < 0.0005$ vs. denervated. Data are expressed as standardized uptake value (SUV), representing radioactive counts per gram of tissue, divided by injected dose of radioactivity per gram of animal weight. (c) Transverse PET images showing ^{11}C-MHED uptake in the iBAT before and after monolateral resection of the SNS fibers innervating BAT. (d) PET/CT analysis of ^{11}C-MHED uptake in sham-operated iBAT lobe of mice pre-treated with vehicle ($n=4$) or desipramine ($n=7$) (10 mg/kg i.p.), 30 min before tracer injection. $^{***}p < 0.0005$ vs. vehicle. (e) Representative photomicrographs showing TH immunoreactivity (arrows) in a sham-operated and in an SNS-denervated iBAT lobe. Magnification, $\times 40$.

^{11}C-MHED, animals were repeatedly imaged at different time points (5, 10, 20, 30, 40, 60 or 80 min) after tracer injection. No anesthesia was used during the ^{11}C-MHED biodistribution phase preceding each scan.

To analyze the specificity of the PET signal, a selective surgical denervation of the SNS fibers innervating the left pad of iBAT was performed. The right BAT pad was sham-operated and used as an internal control. As opposed to the sham-operated BAT lobe, PET/CT imaging did not detect any significant signal in the denervated BAT pad (Figure 1b and c). The accumulation of ^{11}C-MHED reached a plateau at 30 min after injection in the sham-operated pad, in which standardized uptake values (SUVs) were ~3–5-fold higher than in the denervated pad, at all the time points analyzed (Figure 1b).

Acute pre-treatment with the NE reuptake transporter (NET) inhibitor desipramine induced a significant 5-fold reduction in the PET signal in sham-operated pads (Figure 1d), but did not induce any modification in the denervated depots (Figure S1a). The efficiency of the surgical denervation was verified by tyrosine hydroxylase (TH) immunostaining. No immunoreactive fibers could be detected in the denervated BAT pad, whereas these fibers were abundant in the sham-operated pad (Figure 1e). These results show that that PET/CT imaging of ^{11}C-MHED can reveal SNS activity in BAT with a high degree of specificity.

2.2. ^{11}C-MHED is a valid tracer to investigate the SNS-dependent BAT adaptation

Norepinephrine (NE) was widely demonstrated to mediate BAT thermogenic activity and UCP-1 expression in response to environmental temperature acclimation [15,2]. To verify whether ^{11}C-MHED represents an efficient tracer to analyze the SNS-mediated BAT activation, its bio-distribution was studied in animals acclimated at different environmental temperatures. PET/CT scans showed a higher ^{11}C-MHED uptake in BAT of animals kept at 21 °C than in animals studied at 26 °C (Figure 2a). Accordingly, UCP-1 protein levels were higher in BAT of mice analyzed at 21 °C than in those analyzed at 26 °C (Figure S1b).

NE controls BAT activity, mainly through the stimulation of β_3-ARs in brown adipocytes. Thus, we analyzed the ^{11}C-MHED accumulation in BAT of mice chronically treated with CL316,243, a selective β_3–AR agonist (1 mg/kg per day, i.p. injected for 4 weeks). As shown in Figure 2b and Figure S1c, ^{11}C-MHED uptake values and UCP-1 protein

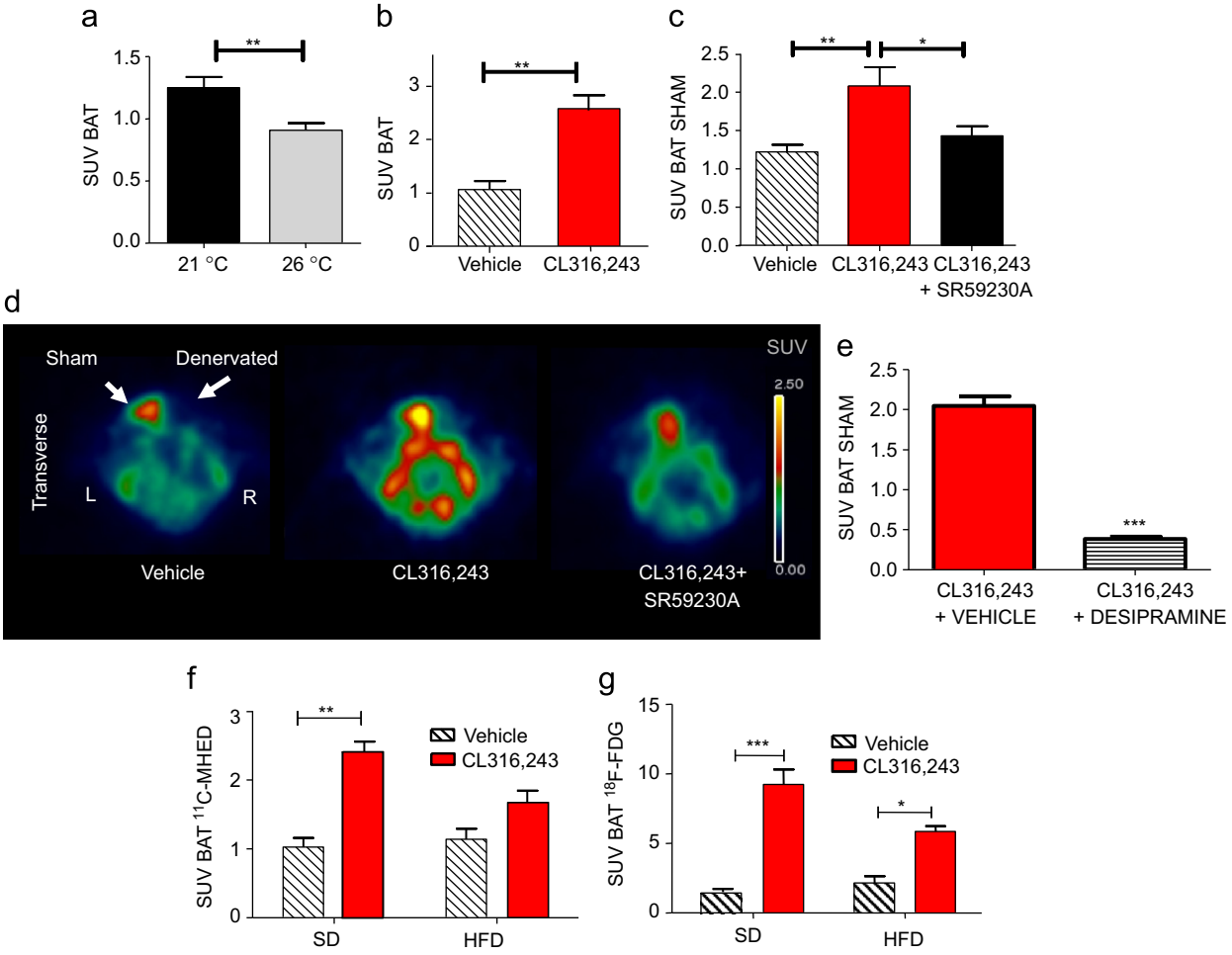

Figure 2: Analysis of ^{11}C-MHED uptake in BAT following experimental activation of SNS. See also Figure S1. (a) Analysis of ^{11}C-MHED uptake in iBAT of mice acclimated either at 21 °C ($n=8$) or 26 °C for 3 months ($n=9$). $^{**}p<0.005$ vs. vehicle. (b) Analysis of ^{11}C-MHED uptake in iBAT of animals chronically treated either with vehicle ($n=5$) or CL316,243 ($n=6$, 1 mg/kg per day, i.p.) for 4 weeks. $^{**}p<0.005$ vs. vehicle. (c) Analysis of ^{11}C-MHED uptake in sham-operated iBAT lobe of mice ($n=5$) by three repeated PET/CT scans (1 week of recovery between the scans) performed after vehicle, CL316,243, or CL316,243 + SR59230A acute administration. $^{**}p<0.005$ vs. vehicle $^{*}p<0.05$ vs. CL316,243. CL316,243 (1 mg/kg i.p.) was injected 1 h before tracer administration. SR59230A (5 mg/kg per os) pre-treatment was performed 1 h before CL316,243 injection. (d) Representative PET image showing ^{11}C-MHED accumulation in sham-operated and SNS-denervated iBAT lobe (arrows) of a representative mouse treated as in Figure 2c. (e) PET/CT analysis of ^{11}C-MHED uptake in sham-operated iBAT lobe of mice treated with CL316,243 (1 mg/kg i.p.) and subsequent (30 min later) injection of vehicle ($n=5$) or desipramine ($n=5$) (10 mg/kg i.p.). Tracer was injected 1 h after CL316,243 administration. $^{***}p<0.0005$ vs. vehicle. (f) Analysis of ^{11}C-MHED uptake in iBAT of SD ($n=5$) and HFD ($n=5$) mice by two repeated PET/CT scans, performed following acute (1 h) treatment either with vehicle or CL316,243 (1 mg/kg i.p.). $^{***}p<0.0005$ vs. SD vehicle by Bonferroni post test. 2-way ANOVA shows significant interaction between diet type and treatment ($p<0.05$) and accounts for approximately 11,74% of the total variance with $F=7.958$. Diet accounts for approximately 6.20% of the total variance with $F=4203$. Treatment accounts for approximately 58.46% of the total variance with $F=39.63$. (g) Analysis of ^{18}F-FDG uptake (SUV) in iBAT of lean SD and HFD mice as in Figure 2 f. $^{***}p<0.0005$ vs. SD vehicle, $^{*}p<0.05$ vs. HFD vehicle by Bonferroni post test. 2-way ANOVA shows significant interaction between diet type and treatment ($p<0.01$) and accounts for approximately 6.71% of the total variance with $F=7.78$. Diet accounts for approximately 61.09% of the total variance with $F=70.86$. Treatment accounts for approximately 6.51% of the total variance with $F=7.55$.

levels were higher in the BAT of CL316,243-treated animals, as compared with vehicle treated mice.

To analyze whether ^{11}C-MHED uptake in BAT is affected by the acute modulation of SNS-mediated thermogenesis, mice with monolateral BAT sympathectomy were treated with CL316,243 (1 mg/kg), and scanned by PET/CT 1 h after injection of the agonist. The acute treatment with CL316,243 induced a significant increase in ^{11}C-MHED uptake in the sham-operated, but not in the denervated BAT pad. This increased uptake was blocked by SR59230A, a selective β_3-AR antagonist [16], as administered orally (5 mg/kg) 1 h before CL316,243 (Figure 2c and d), and was also blocked by desipramine administration (Figure 2e). No significant modification in ^{11}C-MHED uptake was observed following either SR59230A, or CL316,243 plus SR59230A treatment in the SNS-denervated BAT moiety (Figure S1d). Altogether, these results suggest that ^{11}C-MHED PET/CT imaging can effectively provide information on both acute and chronic changes in SNS-dependent BAT thermogenesis.

2.3. Analysis of ^{11}C-MHED uptake in the BAT of diet-induced obese mice

The effect of DIO on SNS activity in BAT has been investigated with different experimental approaches, although conclusive results are lacking [2]. To verify the usefulness of the novel imaging technology in this context, we performed ^{11}C-MHED PET/CT experiments in mice fed with a standard chow diet (SD) or with a high-fat diet (HFD, 60% of calories derived from fat). At the end of the specific dietary regimen, mice were PET/CT scanned either after acute (1 h) vehicle or CL316,243 (1 mg/kg) treatment. As shown in Figure 2f, CL316,243 induced a significant increase in the BAT ^{11}C-MHED uptake of SD mice, but not of HFD-fed mice (Figure 2f).

To investigate whether the reduced stimulatory effect of CL316,243 on ^{11}C-MHED uptake in HFD mice was paralleled by a decreased BAT activity, ^{18}F-FDG PET/CT scans were performed using the same experimental setting as in Figure 2f. As shown in Figure 2g and Figure S1d, although no differences could be detected in the ^{18}F-FDG uptake between the vehicle-treated SD and HFD mice, a lower β_3-AR agonist-induced ^{18}F-FDG uptake was observed in BAT of HFD- than SD-fed mice. These results suggest that the HFD induces a defective BAT response to acute β_3-AR stimulation.

2.4. *In vivo* analysis of WAT to BAT conversion by ^{11}C-MHED PET/CT

Previous studies have shown that chronic CL316,243 administration leads to the appearance of cluster of brown adipocytes within WAT of rodents [17,18]. To assess the potentiality of PET/CT imaging to capture WAT to BAT transformation, C57BL6 mice fed with SD diet were chronically treated with CL316,243 (1 mg/kg daily i.p.) or vehicle, for 4 weeks. ^{11}C-MHED and ^{18}F-FDG uptake in the inguinal subcutaneous (i.s.) WAT was imaged after 4 weeks of treatment. The same animals were also 'ad interim' analyzed after 3 weeks of treatment. At the end of the scanning sessions, mice were sacrificed and WAT to BAT conversion analyzed *ex-vivo* in the WAT depots that had been imaged.

As shown in Figure 3a, PET/CT imaging revealed the presence of ^{11}C-MHED dense areas in the i.s. WAT depots of mice treated with CL316,2434 for 4 weeks. CT scans confirmed that the PET signal was located in WAT (Figure 3a). Notably, the same ^{11}C-MHED avid areas were detected by ^{18}F-FDG-PET (Figure 3a). No accumulation of ^{11}C-MHED and ^{18}F-FDG was observed in i.s. WAT depots in mice treated with vehicle (Figure S2a). Quantitatively, both ^{11}CMHED and ^{18}FFDG uptake rates in the left i.s. WAT depot were twice as high as in the CL316,243-treated mice than in the vehicle-treated mice after 3 weeks of drug administration (Figure 3b and c). A more pronounced (*i.e.*, 3-fold) increase in the signal was seen in i.s. WAT after 4 weeks of CL316,243 versus vehicle treatment (Figure 3b and c). The ^{11}C-MHED SUV values in the bladder of CL316,243- and vehicle-treated mice were similar (Figure S2b), indicating that the differences observed in the i.s. WAT could not be accounted for by the spill-over of radioactivity from the bladder.

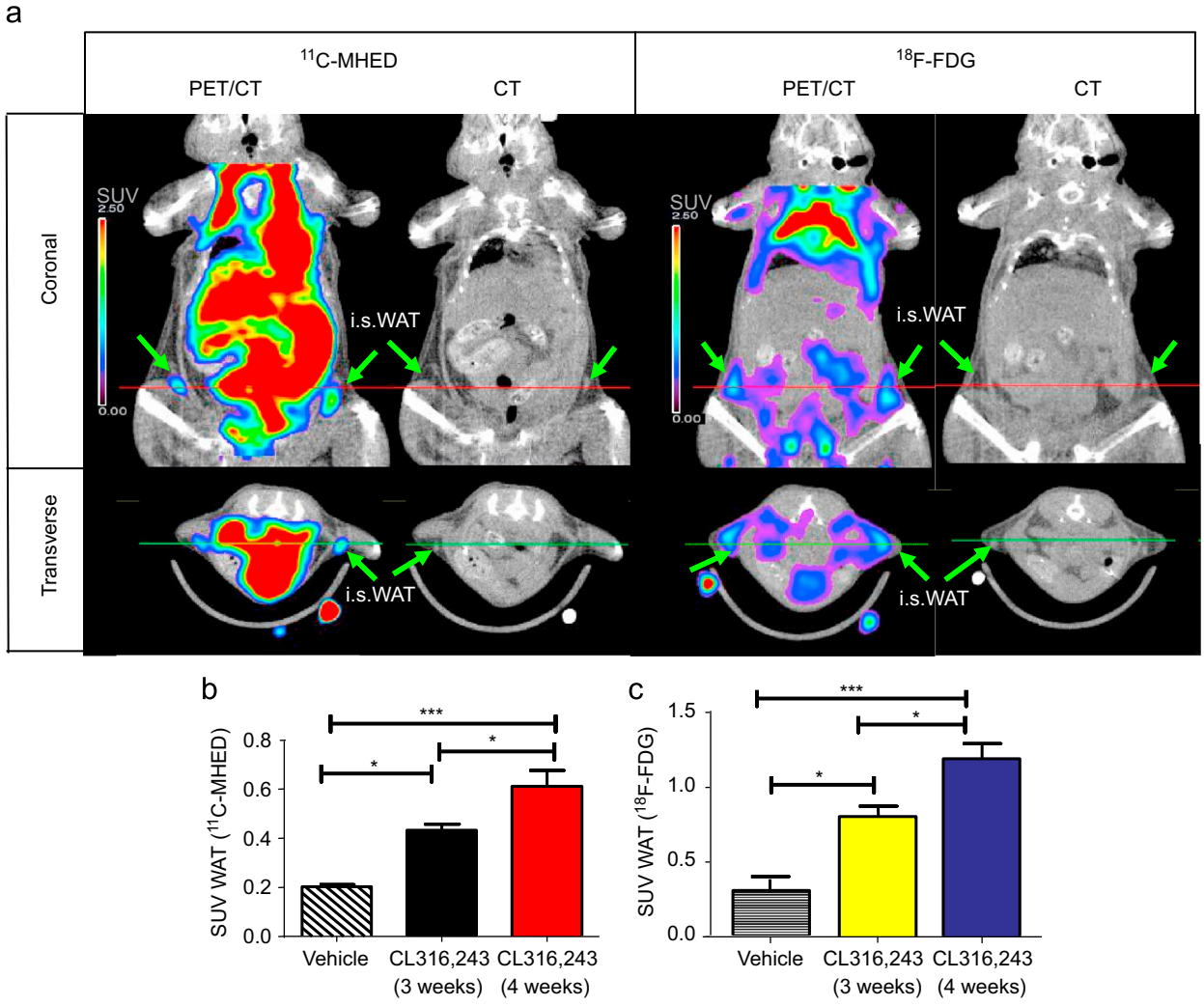

Figure 3: PET/CT imaging of WAT following treatment with a $_3$-AR agonist. See also Figure S2. (a) Coronal (top) and transverse (bottom) views of PET/CT fused (left) and CT (right) images showing ^{11}C-MHED and ^{18}F-FDG accumulation in the i.s. WAT (arrows) of a representative mouse chronically treated with CL316,243 for 4 weeks. Radioactive counts are expressed as SUV. Red lines indicate the image sections reported in the transverse views. (b) Analysis of ^{11}C-MHED uptake in the i.s. WAT of mice chronically treated with vehicle (n=5) or with CL316,243 (n=6), and analyzed by PET/CT imaging after 3 weeks or 4 weeks of CL316,243 administration. ****$p < 0.0005$ vs. vehicle; *$p < 0.05$ vs. vehicle or CL316,243 (3 weeks). SUV values for mice treated for 3 and 4 weeks with vehicle were cumulated since they were not statistically different. (c) Analysis of ^{18}F-FDG uptake in WAT of the animals in which we obtained the results shown in Figure 3b, after 3 weeks or 4 weeks of CL316,243 administration. ***$p < 0.0005$ vs. vehicle; *$p < 0.05$ vs. vehicle or CL316,243 (3 weeks). SUV values for mice treated for 3 and 4 weeks with vehicle were cumulated since they were not statistically different. (For interpretation of the references to color in this figure legend, the reader is referred to the web version of this article.)

Finally, the *ex vivo* analyses confirmed that 4-week CL316,243 treatment was able to convert WAT into a SNS-competent brown fat-like tissue. First, the UCP-1 and peroxisome-proliferator activated receptor γ co-activator 1 α (PGC-1α) mRNA and protein (UCP-1) levels were higher in WAT of mice treated with CL316,243 as compared to those treated with the vehicle (Figure 4a–c). Second, histological examinations identified BAT-like tissue, with clusters of multilocular adipocytes, in the i.s. WAT after CL316,243 treatment (Figure 4d). Moreover, CL316,243 increased the TH-positive parenchymal nerve fibers in i.s. WAT (Figure 4d). Importantly, image analysis of WAT density by CT scan confirmed the histological and molecular data. In fact, CT Hounsfield Unit (HU) values in the i.s. WAT regions were significantly higher (*i.e.*, higher density) after 3 weeks of CL316,243 treatment than in vehicle-treated mice, and a more pronounced increase in i.s. WAT HUs was observed after 4 weeks of treatment (Figure S2c).

Altogether, our findings document that PET/CT imaging is an effective tool for non-invasive study of the SNS activation of BAT, and the white-to-brown fat cell conversion in i.s. WAT after chronic β_3-AR stimulation.

3. DISCUSSION

A large body of preclinical evidence indicates that BAT thermogenetic activity is mainly regulated by the SNS [19,20] specifically by NE action on β_3-AR receptors expressed on adipocytes surface [2]. The SNS is also a potent regulator of brown adipocyte proliferation and differentiation in rodents [10].

The present study was aimed at (i) validating the use of ^{11}C-MHED PET/CT imaging to study SNS function in BAT and (ii) investigating the efficiency of PET/CT imaging to trace the white-to-brown fat conversion in *in vivo* experimental settings.

^{11}C-MHED is a positron emitting NE analogue, so far exclusively employed in the characterization of SNS function in the myocardium by PET imaging. Because it cannot be easily metabolized, ^{11}C-MHED accumulates in sympathetic neurons, providing a PET signal that is proportional to local NE turnover [21]. This tracer has also been shown (in *ex-vivo* studies) to specifically accumulate in BAT [13] and we have recently reported the first example of ^{11}C-MHED PET images of BAT, detecting an increased ^{11}C-MHED accumulation in brown fat of genetically modified mice with a high peripheral SNS tone [22]. In the present study, we provide the first evidence that ^{11}C-MHED PET/CT imaging represents a novel *in vivo* approach to study SNS activity in BAT. Indeed, monolateral SNS denervation unequivocally demonstrated that ^{11}C-MHED accumulation is specific for the sympathetic innervation of BAT. Moreover, ^{11}C-MHED uptake in the BAT was fully dependent on the activity of the neuronal transporter NET, providing further evidence of the neuronal nature of the signal detected by PET.

Noteworthy, ^{11}C-MHED accumulation in BAT was proportional to the local level of SNS-induced BAT activity. In fact, when SNS-induced thermogenesis in BAT was modified by exposing the animals to different environmental temperatures, the expected modification in ^{11}C-MHED uptake was observed. Moreover, in the light of the notion that SNS dependent thermogenesis is mainly due to NE action on β3ARs expressed on adipocytes, we also studied ^{11}C-MHED uptake in the BAT of animals treated with the selective β3AR agonist CL316,243. We chose not to test the effect of NE infusion directly, because the competition between the labeled and the unlabeled molecules would have led to an underestimation of ^{11}C-MHED uptake. The data obtained with this set of experiments showed that acute or chronic modifications in BAT thermogenesis induced by CL316,243, were accompanied by a specific neuronal ^{11}C-MHED accumulation in the tissue. On one hand, these data indicate that ^{11}C-MHED PET/CT is a promising approach to quantify acute and chronic modifications in SNS-mediated thermogenesis in BAT. On the other hand, they imply a broader biological interpretation. Indeed, β_3-ARs are mainly, albeit not only, expressed in brown and white adipocytes [23]. Thus, the increase in ^{11}C-MHED uptake observed in BAT sympathetic neurons after β_3-ARs agonism suggests that, when activated, brown adipocytes are able to modulate the activity of the local parenchymal sympathetic nerves located in the BAT. However, because a limited amount of β_3-ARs may be expressed also in neurons [24] our findings do not fully rule out that the direct stimulation of β_3-AR in SNS neurons may, at least in part, explain our results.

Intriguingly, the β_3-AR agonist-induced BAT ^{11}C-MHED uptake in DIO mice was significantly lower when compared to that of SD-fed mice. The defect in SNS activity paralleled the impairment in BAT activation by CL316,243, as shown by ^{18}F-FDG uptake values in corresponding BAT regions of obese mice. These data highlight that an impaired SNS-brown adipocyte cross-talk underlies the reduced thermogenic potential of this tissue in obesity, and that this defect can be monitored and measured by PET/CT imaging.

In the light of the data showing that PET/CT imaging of BAT ^{11}C-MHED accumulation is a valid tool to quantify SNS signaling in typical BAT depots, we also aimed to demonstrate that PET/CT imaging is able to visualize and measure the functional activity of newly generated brown adipose cells in the inguinal subcutaneous WAT. When WAT to BAT conversion was promoted by the chronic treatment with a β_3-AR agonist, a clear-cut, hyper-intense ^{11}C-MHED and ^{18}F-FDG signal could be detected and quantified in WAT. Noteworthy, progressively higher ^{11}C-MHED and ^{18}F-FDG uptake values were observed after 3 weeks and 4 weeks of β_3-AR agonist treatment, suggesting that tracers accumulation is proportional to the amount of newly generated brown adipose cells in WAT. A significant amount of ^{11}C-MHED and ^{18}F-FDG uptake was observed in non-adipose sites located in the visceral cavity, such as the bladder, the liver and the gastrointestinal tract. This extra adipose labeling limits the possibility to visualize and analyze the phenomenon of browning in the visceral adipose tissue. Because of its favorable anatomical localization, the inguinal subcutaneous WAT is less affected by the effect of spill-over radioactivity from non adipose sites. These properties make the inguinal WAT an ideal depot for the analysis of browning by PET/CT imaging. Future studies will be needed to address whether *de novo* generated BAT can be quantified and visualized by PET/CT imaging in adipose depots located in the visceral cavity.

To our knowledge, these findings represent the first evidence of the *in vivo* detection of white-to-brown fat transdifferentiation by non-invasive imaging, and support the biological notion that white adipocytes, under appropriate conditions, can give rise to functionally active (as revealed by the increased ^{18}F-FDG signal) and SNS-competent (as revealed by the increased ^{11}C-MHED signal) brown adipocytes. Moreover, the parallel time-course of accumulation of ^{18}F-FDG and ^{11}C-MHED in WAT during chronic β_3 agonist treatment, suggests that SNS signaling in adipose tissue is importantly involved in the process of transformation of WAT into thermogenetically active BAT. These data support the possibility, as previously suggested by analyzing adipose tissue of chronically cold-exposed mice [11], which SNS activity could actively contribute to regulate the plastic nature of adipose tissue.

The regulation of brown adipose cells differentiation and thermogenesis by the SNS is well established in rodents, but still under debate in humans. Species specific differences in the mechanisms underlying SNS mediated thermogenesis in the BAT may exist between rodents and

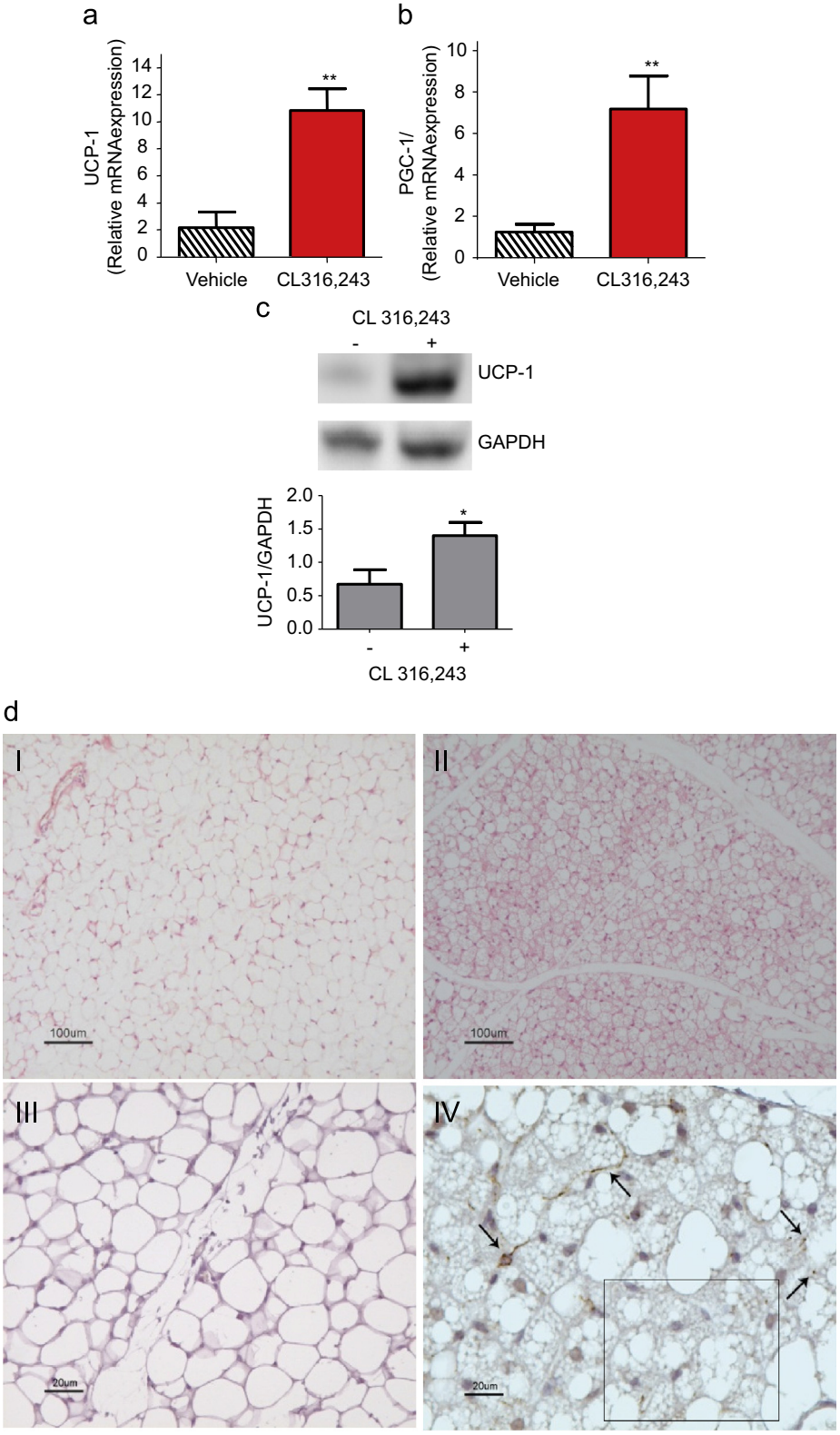

Figure 4: *Ex-vivo* analysis of WAT-to-BAT conversion. (a) UCP-1 mRNA expression analyzed by qPCR in the i.s. WAT, after 4 weeks of vehicle or CL316,243 administration, in the same animals shown in Figure 3b and c. $^{**}p < 0.005$ vs. vehicle. (b) PGC-1 mRNA expression analyzed by qPCR in the i.s. WAT, as in a. $^{**}p < 0.005$ vs. vehicle. (c) Western blot analysis of UCP-1 levels in the i.s. WAT as in a. Relative UCP-1 values for densitometric analysis were determined by normalization for the house-keeping protein GAPDH. (d) H&E staining (top, magnification × 10) and immunohistochemistry for TH (bottom: magnification × 40), in sections of i.s. WAT of mice chronically treated with vehicle (left: I and III) or CL316,243 (right: II and IV) for 4 weeks. Arrows indicate TH-positive parenchymal fibers.

humans [25]. In a recent report, it was shown that mild cold exposure, but not intra-muscular ephedrine injection, induces a specific response by the SNS to activate BAT and increase energy expenditure in humans [26]. This study, which highlights the role of SNS activation in the regulation of human BAT activity, suggests also that specific mechanisms mediated by cold exposure, but not by β_3-ARs activation, may be important for regulation of SNS-mediated thermogenesis in human BAT. In this context, future PET/CT imaging studies using SNS-related PET tracers (such as ^{11}C-MHED) and PET molecules tracing substrates oxidation (such as ^{18}F-FDG or ^{11}C-acetate, as shown in [27]) could provide key information concerning the relationship between SNS signaling and thermogenesis in human BAT.

In conclusion, ^{11}C-MHED is a novel and efficient tracer for the *in vivo* PET/CT characterization of SNS-dependent BAT activity and white-to-brown fat conversion. Our findings have translational value, since the tracer is already available for use in humans.

4. EXPERIMENTAL PROCEDURE

4.1. Materials

Desipramine hydrochloride and CL316,243 were purchased from Sigma-Aldrich and dissolved in 0.9% saline. Synthesis and quality control of ^{11}C-MHED were performed as previously described [21].

4.2. Animals

Twelve-week old C57BL/6J male mice were housed under conditions of controlled temperature (21 °C or 26 °C) for 3 months. During this period, mice were fed with a standard diet or with a high fat diet (60% of calories from fat), as previously described [22]. At the end of 3 months, PET/CT imaging studies were performed. If not otherwise specified, PET/CT data refer to experiments performed at 21 °C. All procedures were approved by the Central Veterinary Service of Bologna University. All experiments were performed in 4 h-fasted animals.

4.3. Monolateral sympathectomy of BAT

Surgical sympathectomy of the interscapular BAT was performed, as previously described [22], by cutting the nerve bundles of the left BAT pad. The right interscapular BAT pad was sham operated and used as an internal control. The quality of the denervation procedure was verified in each animal by tyrosine hydroxylase (TH) immunostaining.

4.4. PET/CT imaging

A PET system (Explore Vista, GE, Milwakee, USA) and a CT system (microCT eXplore Locus, GE) designed for small animals were used. Synthesis and quality control of ^{11}C-MHED were performed as previously described [21].

To examine the ^{11}C-MHED bio-distribution in BAT, mice monolaterally sympathectomized were repeatedly scanned, each one six times, after tail vein injection of ^{11}C-MHED (30 MBq in 300 μl of saline). During each imaging session, animals were analyzed at different time points after tracer injection. No anesthesia was administered after tracer injection, *i.e.* during the phase of ^{11}C-MHED bio-distribution, after which a static PET scan of 10 min was performed under gas sevorane anesthesia (1% of oxygen supplementation), followed by a CT scan. SUV values in BAT images were obtained as previously described [22]. ^{11}C-MHED PET experiments, when not reported otherwise, refer to animals scanned 30 min after the tracer injection.

^{18}F-FDG PET/CT scans were performed as previously described [22]. For the analysis of WAT-to-BAT conversion, ^{18}F-FDG was injected 2 h after the end of the ^{11}C-MHED PET/CT scanning sessions, in animals treated either for 3 or 4 weeks with CL316,243 (1 mg/kg per day, i.p.) or vehicle.

4.5. Real time PCR and immunoblotting

Messenger RNA levels were determined by qPCR analysis, performed by using the iQ Sybr Green Supermix (BioRad, Hercules, California, USA) with iCycler (BioRad) instrumentation and software. For immunoblotting, total tissue lysates were separated by SDS-PAGE, transferred to PVDF membrane and probed with anti-UCP1 and anti-GAPDH antibodies from Abcam (Cambridge, UK). For further details see the Supplementary methods.

4.6. Histology and immunohistochemistry

Tissue specimens underwent standard hematoxylin–eosin staining for morphological analysis. Sections of formalin fixed, paraffin embedded BAT and WAT were stained and revealed using a rabbit polyclonal anti-TH antibody and a commercially available avidin–biotin–immunoperoxidase staining system (Vectastain Elite ABC Kit, Vector Laboratories, USA). For further details see the Supplementary methods.

4.7. Statistics

Student's *t* test or analysis of variance (ANOVA) with *Bonferroni post-hoc* test were used. The software GraphPad Prism 5.0 was used. p value less than 0.05 were considered statistically significant. Data are expressed as mean $\pm$ SEM.

ACKNOWLEDGEMENTS

This work was supported by a grant from MIUR PRIN 2010-2011 Project 2010329EKE_004 to UP.

CONFLICT OF INTEREST

None.

APPENDIX A. SUPPORTING INFORMATION

Supplementary data associated with this article can be found in the online version at http://dx.doi.org/10.1016/j.molmet.2013.04.002.

REFERENCES

[1] Rothwell, N.J., and Stock, M.J., 1979. A role for brown adipose tissue in diet-induced thermogenesis. Nature 281:31–35.

[2] Cannon, B., and Nedergaard, J., 2004. Brown adipose tissue: function and physiological significance. Physiological Reviews 84:277–359.

[3] Feldmann, H.M., Golozoubova, V., Cannon, B., and Nedergaard, J., 2009. UCP1 ablation induces obesity and abolishes diet-induced thermogenesis in mice exempt from thermal stress by living at thermoneutrality. Cell Metabolism 9:203–209.

[4] Cederberg, A., Grønning, L.M., Ahrén, B., Taskén, K., Carlsson, P., and Enerbäck, S., 2001. FOXC2 is a winged helix gene that counteracts obesity, hypertriglyceridemia, and diet-induced insulin resistance. Cell 106:563–573.

[5] Bartelt, A., Bruns, O.T., Reimer, R., Hohenberg, H., Ittrich, H., Peldschus, K., et al., 2011. Brown adipose tissue activity controls triglyceride clearance. Nature Medicine 17:200–205.

[6] Seale, P., Conroe, H.M., Estall, J., Kajimura, S., Frontini, A., Ishibashi, J., et al., 2011. Prdm16 determines the thermogenic program of subcutaneous white adipose tissue in mice. Journal of Clinical Investigation 121:96–105.

[7] Cypess, A.M., Lehman, S., Williams, G., Tal, I., Rodman, D., Goldfine, A.B., et al., 2009. Identification and importance of brown adipose tissue in adult humans. New England Journal of Medicine 360:1509–1517.

[8] Van Marken Lichtenbelt, W.D., Vanhommerig, J.W., Smulders, N.M., Drossaerts, J.M., Kemerink, G.J., Bouvy, N.D., et al., 2009. Cold activated brown adipose tissue in healthy men. New England Journal of Medicine 360:1500–1508.

[9] Virtanen, K.A., Lidell, M.E., Orava, J., Heglind, M., Westergren, R., Niemi, T., et al., 2009. Functional brown adipose tissue in healthy adults. New England Journal of Medicine 360:1518–1525.

[10] Cinti, S., 2001. The adipose organ: morphological perspectives of adipose tissues. Proceedings of the Nutrition Society 60:319–328.

[11] Cinti, S., 2011. Between brown and white: novel aspects of adipocyte differentiation. Annals of Medicine 43:104–115.

[12] Kajimura, S., and Seale, P., 2010. Spiegelman BM.Transcriptional control of brown fat development. Cell Metabolism 11:257–262.

[13] Thackeray, J.T., Beanlands, R.S., and Dasilva, J.N., 2007. Presence of specific ^{11}C-meta-hydroxyephedrine retention in heart, lung, pancreas, and brown adipose tissue. Journal of Nuclear Medicine 48:1733–1740.

[14] Lin, S.F., Fan, X., Yeckel, C.W., Weinzimmer, D., Mulnix, T., Gallezot, J.D., et al., 2012. *Ex vivo* and *in vivo* evaluation of the norepinephrine transporter ligand [(11)C]MRB for brown adipose tissue imaging. Nuclear Medicine and Biology. [Epub ahead of print].

[15] Nedergaard, J., Golozoubova, V., Matthias, A., Asadi, A., Jacobsson, A., and Cannon, B., 2001. UCP1: the only protein able to mediate adaptive non-shivering thermogenesis and metabolic inefficiency. Biochimica et Biophysica Acta 1504:82–106.

[16] Nisoli E., Tonello C., Landi M., and Carruba M.O., 1996. Functional studies of the first selective beta 3-adrenergic receptor antagonist SR 59230A in rat brown adipocytes. Mol. Pharmacol. 49:7–14.

[17] Himms-Hagen, J., Melnyk, A., Zingaretti, M.C., Ceresi, E., Barbatelli, G., and Cinti, S., 2000. Multilocular fat cells in WAT of CL-316243-treated rats derive directly from white adipocytes. American Journal of Physiology Cell Physiology 279, C670–81.

[18] Inokuma, K., Okamatsu-Ogura, Y., Omachi, A., Matsushita, Y., Kimura, K., Yamashita, H., et al., 2006. Indispensable role of mitochondrial UCP1 for antiobesity effect of beta3-adrenergic stimulation. American Journal of Physiology—Endocrinology and Metabolism 290:E1014–E1021.

[19] Richard, D., Carpentier, A.C., Doré, G., Ouellet, V., and Picard, F., 2010. Determinants of brown adipocyte development and thermogenesis. International Journal of Obesity (London) 34 (Suppl 2), S59–S66.

[20] Whittle, A.J., López, M., and Vidal-Puig, A., 2011. Using brown adipose tissue to treat obesity-the central issue. Trends in Molecular Medicine 17:405–411.

[21] Rosenspire, K.C., Haka, M.S., Van Dort, M.E., Jewett, D.M., Gildersleeve, D.L., Schwaiger, M., et al., 1990. Synthesis and preliminary evaluation of carbon-11-meta-hydroxyephedrine: a false transmitter agent for heart neuronal imaging. Journal of Nuclear Medicine 31:1328–1334.

[22] Quarta, C., Bellocchio, L., Mancini, G., Mazza, R., Cervino, C., Braulke, L.J., et al., 2010. CB(1) signaling in forebrain and sympathetic neurons is a key determinant of endocannabinoid actions on energy balance. Cell Metabolism 11:273–285.

[23] Ursino, M.G., Vasina, V., Raschi, E., Crema, F., and De Ponti, F., 2009. The beta3-adrenoceptor as a therapeutic target: current perspectives. Pharmacological Research 59:221–234.

[24] Summers, R.J., Papaioannou, M., Harris, S., and Evans, B.A., 1995. Expression of b3-adrenoceptors in rat brain. British Journal of Pharmacology 116:2547–2548.

[25] Nedergaard, J., and Cannon, B., 2010. The changed metabolic world with human brown adipose tissue: therapeutic visions. Cell Metabolism 11:268–272.

[26] Cypess, A.M., Chen, Y.C., Sze, C., Wang, K., English, J., Chan, O., et al., 2012. Cold but not sympathomimetics activates human brown adipose tissue *in vivo*. Proceedings of the National Academy of Sciences 109:10001–10005.

[27] Ouellet, V., Labbé, S.M., Blondin, D.P., Phoenix, S., Guérin, B., Haman, F., et al., 2012. Brown adipose tissue oxidative metabolism contributes to energy expenditure during acute cold exposure in humans. The Journal of Clinical Investigation 122:545–552.

